# High-Resolution Imaging Integrated Approach to Enhance Pay Count and Turbidites Reservoir Architecture, Offshore Nile Delta, Egypt*

**El-Saied M. Felifel[1], Mohamed Fathy[2], Abdel Moneim El Araby[3], Elie Haddad[1], Mohamed Nassar[1], and Moustafa Mounir[2]**

Search and Discovery Article #20274 (2014)
Posted October 13, 2014

*Adapted from extended abstract prepared in conjunction with poster presentation given at AAPG International Conference & Exhibition, Istanbul, Turkey, September 14-17, 2014, AAPG © 2014

[1]Schlumberger, Cairo (ehassan4@slb.com)
[2]GDF Suez
[3]Cairo University

## Abstract

Offshore Egypt has one of the most promising gas fields in the world, representing deepwater turbidite proximal channel sands and distal thinly bedded turbidities sands. Evaluating reservoirs in thinly bedded formations remains an extremely challenging process. We explore one method of improving how such reservoirs are characterized, which involved integrating conventional openhole logs with high-resolution microresistivity images to reveal reservoir complexity. Reservoir delineation, architecture, and accurate pay count were the main challenges faced in this study.

Detailed high-resolution electrofacies analysis has been extracted for better understanding of offshore Nile Delta wells drilled in the Abu Madi and Kafr-El Sheikh formations. The studied Late Miocene- Pliocene succession shows an overall retrogradational pattern and a fining-upward depositional motif. Twelve main facies associations and sedimentary units are identified. The basal sedimentary unit is equivalent to Messinian Abu Madi Formation and represents a sandy estuarine complex facies association. It was succeeded by Early Pliocene Kafr El Sheikh Formation, where submarine channel fill- levee complex prevailed. It developed during a flooding event and relative rise in eustatic sea-level. The intervening silty heterolithics, laminated siltstone, and massive claystone with rare sandstone interbeds represent proximal to a distal levee depositional suite. The laminated siltstones in these levee deposits are locally gas-bearing.

Understanding high-resolution single-well sedimentary facies, along with accurately quantifying pay count using different approaches, have improved the overall picture of the depositional regime. Sedimentary analysis using image logs helped to illustrate reservoir architecture for better sand delineation and accurate reserve estimation. Pressure points and samples have been taken over the potential thin-bedded turbiditic channel levee complex, and it shows the presence of gas in this unit. As a result of these integrated analyses, twenty meters of thin-bedded

channel levee complex has been perforated and proved to be a gas-bearing zone. Perforation results revealed the productivity and economic potential of the added thin-bedded reservoir pay.

## Introduction

The studied prospect lies in the northern part of the West El-Burullus Offshore concession area, about 65 km from El-Burullus Lake. The water depth ranges from 15 m southwards to 650 m in northwest corner of the field. It is located approximately 15 km south east of Taurus and Libra gas fields and approximately 7 km southwest of Sequoia Gas Field. The West El Burullus Offshore concession covers an area of 726 $km^2$ in the western side of the offshore Nile Delta (Figure 1). The studied prospect consists of several geological events composed mainly of deep marine canyons, which are made of several slope fans. These incised canyons have been formed as a result of major regressive event followed by successive and alternating transgressive and regressive cycles. There are also two targets allocated within the Late Miocene fluvial valleys that were deposited within the shelf area after the Messinian salinity crisis. They are considered part of the mega Abu Qir fluvial system.

The exploration activity in the studied field commenced with drilling the first well targeting Pliocene slope channel turbidites complex of Kafr El Sheikh Formation and Messinian Fluvio-Marine channels of Abu Madi Formation (Figure 2). The presence of gas in the studied reservoir is supported by a seismic amplitude anomaly. On a cross section, it shows typical lenticular geometries of a channel-levee complex (Figure 3).

## Methodology and Available Data

An integrated geological and petrophysical approach has been introduced to properly identify all the potential reservoir zones in the field. Full understanding of the reservoir texture, geometry, architecture and delineation is particularly for characterizing these challenging reservoirs.

All available data, conventional open hole logs (neutron, density, resistivity and gamma-ray), high-resolution micro-resistivity images, continuous core image, and interpreted seismic lines have been integrated together to come up with the detailed workflow described below. The workflow of this study mainly focused on introducing all the answers that can be obtained using high-resolution micro-resistivity images.

### High Resolution Formation Micro-resistivity Image Processing

One of the main steps in the image processing workflow is data normalization, where the image is enhanced prior to the graphical display by histogram modification. The histogram equalization is a technique that aims to enhance the depiction of details in an image by optimizing the usage of colors. The histogram is divided into 64 color classes; dark colors are given for features of the lowest resistivity and white colors for those having the highest ranges of resistivity. Bounded between the highest and lowest resistivity classes, variation in resistivity is displayed by different shades of white, yellow, orange, and black. The results of the image normalization are static and dynamic images according to the type of the window used.

**Static Image Generation**

This phase involves carrying out a single computation in a window covering the entire depth interval specified by the user. Static normalization optimizes the use of colors globally over the specified interval. Locally, there may be intervals where few colors are used, leading to an indistinct image. However, the relationship between color and tool response is the same over the entire image. Static normalized images are best suited for large-scale resistivity variations associated with change in lithology and water or hydrocarbon saturation. Such images mask minor features having low resistivity contrast like hair line fractures, cross bedding, minor slumps, diagenetic variation, and rock fabric.

**Dynamic Image Generation**

In this phase, separate computations are repeated at regularly spaced positions over the user specified depth interval, using a user specified sliding window of relatively short length. This process simulates normalization by a continuous movement of the window. Dynamic normalization locally optimizes the use of colors and is preferred when observing fine image features. Up to a point, the shorter the window length, the greater the enhancement of details. The image resulted from this normalization was used to identify minor features with a very little resistivity contrast with the matrix or host rock, such thin lamination, cross lamination, cross-beds, hairline fractures, textural variations, rock fabric, vugs, and bioturbation. While static images are more convenient in correlation with other logs, both the static and dynamic images complement each other, and both are used together for dip picking.

**Manual Dip Picking and Classification**

Sedimentary and structural dip features were manually picked using a sliding sinusoid. These sinusoids were fitted to planar or sub-planar features that cut the borehole. The lowest point on the sinusoid trough defines the dip azimuth, and the amplitude of the sinusoid defines the dip magnitude (assuming a vertical hole). Sedimentary dips were defined as those resulting from depositional processes and include bed boundaries (planar bed tops and bases, uneven erosional contacts) and internal bedding features (e.g. internal sand lamination, cross lamination, cross bedding, heterolithics lamination, and mud lamination). Structural features include those planes that cut across bedding (fractures, faults). Moreover, the in-situ stresses can be identified through picking and defining the orientation of induced fractures and breakouts. Induced fractures represent the direction of the present day maximum horizontal stress whereas the breakouts represent the direction of the present day minimum horizontal stress.

**Sand Count**

The sand count has been performed over the studied formations using two methods: the simple cut-off method, and the statistical quantitative method.

**1) Simple SRES Cut-Off Method**

In this method the scaled micro resistivity curve (SRES) is used as an input with applying single or multiple resistivity cut offs. In the studied case; SRES curve has been used with 0.2-inch (5 mm) vertical resolution as an input with other logs, such as clay volume and density, to reflect the heterogeneity present, especially in the thinly bedded reservoirs. Due to the intensive facies variation of facies present within the offshore Nile Delta from massive slope channel facies, channel levee thin beds, sandy to silty, and shaly lithologies; multiple cut offs has been applied. In the sandy section that shows a neutron-density cross over (blocky log motif), it is expected to exclude the silty or shaly streaks that are not seen by the conventional openhole logs. In shaly or silty intervals, the sandy streaks which are beyond the vertical resolution of the conventional neutron, density and resistivity logs will be included in the pay count (Figure 4). This method works fine with the perfect homogeneous laminated reservoirs where the anomalies were crossed by all buttons of the high-resolution micro-resistivity images tool.

**2) Statistical Quantitative Method**

In this method the software analyze the micro resistivity range of the whole interval in to a histogram and based on the user preferences; number of bins or cutoffs can be placed based on the histogram distribution which will turn subdivide the facies into number of classes according to the number of bins used (Figure 5). This method represents a volume count as well, honoring the lamination shape across the full circumference of the hole, it is not based only one curve SRES from single button or pads, it is a spectrum analysis of the image in 360 deg, this would honor the heterogeneous lithology like the shaly sand, bioturbated and mottled and this is what makes this method way better than the first method. Thickening and thinning upward sequences can be clearly defined after performing the sand count. These sequences will help in defining the facies stacking patterns while building the facies associations for interpreting the depositional setting.

**Sand Textural Analysis (SandTex)**

The bore hole image resistivity distribution can be visualized as a histogram or variable density log (VDL) display for better visualization of the data. Using this method, the total image resistivity spectrum in a 1-inch interval around the well bore will be analyzed. Hence, the rock textural changes can be digitally analyzed. A pseudo grain sorting index is calculated from the percentile resistivity distribution of the image spectrum. The unimodal distribution of these histograms reflects well-sorted facies and the bimodal to poly modal distribution of the histogram reflects medium to poorly sorted facies (Figure 6). Continuous grains sorting index log can be derived from these histogram distributions and the poor and clean sand facies can be distinguished. These outputs, sorting-index, fractional resistivities, variability, along with layering measurements, and associated open-hole log data can be combined to compute a facies description that captures the textural content of these siliciclastic environments.

**Facies Analysis**

Within this step, the processed images are analysed carefully with high vertical scale compared to core-like description, where actually we deal with image like a core, and every single primary structure is assigned besides the very detailed facies picking. Integrating results of the manual dip picking and the sand textural analysis along with the core data beside the manual electro-facies. The facies are studied further to analyze the

texture, fabric, nature of bed boundaries, internal cyclicity, bed thickness, and internal structures (depositional, biogenic, and deformational). After extracting the facies units, these units could be stacked together to form the facies stacking pattern or the facies association. All the previously mentioned steps are used and integrated together along with the core data, and thin sections (petrography) is available to finally come up with these types of calibrated electro facies.

### Depositional Environment Interpretation

This step represents the most critical part; where the studied facies association output from the previous step, will be analyzed and interpreted in terms of depositional environment. Starting with present-days analogues observed, the past depositional environment of the rock will be interpreted. See Figure 7 below that shows the work flow as a simplified diagram.

## Sedimentary Features Analysis

### Bed Boundaries

These dips include any layers that represent shale or carbonate. They exhibit a low dip magnitude averaging 4.3° and are scattered with a mean azimuth of 147.1°.

### Silt Laminations

Silt lithology was differentiated from sand and shale because the nature of the depositional environment being submarine fans and a general fining of sediment derived from a muddy rich system. Silt laminations occurred throughout most of the interpreted interval as massive or laminated siltstone (Figure 8).

### Sand laminations

Sand laminations were identified based on image texture analysis. They appear resistive if gas filled or conductive if water filled. However, in most intervals, sand grains could be discerned from the image. Some intervals were composed of fine sand, and its texture was not clear. Average dip magnitude was 2.3° while mean azimuth direction was 230.5°.

### Soft Sediment Deformation/Wavy Bedding

Deformed beds occur in some intervals and are primarily due to slumping associated with mud-rich turbidite systems; when there is a contrast in densities between layers, such as sand and mud, one lithology slumps into the other. This also indicates the presence of water in the system and presents in the form of water escape structures. Wavy bedding is evident in certain intervals and indicates the action of waves on the sediments. Soft sediment deformations were also recorded as a result of the compaction or the onset slope failure (Figue 9).

### Scour Surface/Internal Erosive Surface

A few scour surfaces were picked at the base of sandstone intervals. They represent the initial erosive power that comes with the increase of grain size in a system. There were a couple of internal erosive surfaces as well, indicating an amalgamated sandstone pattern.

### Inclined Heterolithic Stratification

Alternating, thinly laminated, millimeter scale layers of sand and silt dipping toward the axis of the channels (perpendicular to the flow).

### Cross Lamination

These laminations appear in both sand and silt lithology and represent a higher energy flow than sand or silt laminations alone. This results in a higher angle of deposition than the heterolithic dips.

### Formation Micro-Resistivity Facies Calibration

The electro facies generated from the FMI has been calibrated to the core facies and both are matching very well. The sorting index generated from the sandTex* showed generally medium to well sorted sandy facies which are quite similar to the results of the grain size analysis from the core (Figure 10).

## Sedimentological Interpretation

Detailed interpretation of depositional environments was carried out across the Abu Maddi Formation and Pliocene Kafr El Sheikh Formation. Interpretation was based on lithofacies characteristics, sedimentary structures, depositional dip change, significant depositional surfaces, and depositional motif of the highresolution micro resistivity borehole images. The interpreted lithofacies were assembled into lithofacies associations which reflect the depositional building-blocks and vertical facies change in terms of an overall depositional model of the studied succession.

The high resolution micro-resistivity image was integrated with a lithological description of the mud log, biostratigraphic data as well as calibrated with core data. Sedimentary dip types were used in order to define lithofacies, depositional packages and to determine paleocurrent orientations. The interpreted facies associations and their detailed lithofacies characteristics and depositional regimes will be discussed from base to top in the below section.

## Abu Madi Formation Depositional Facies Characteristics

Thick intercalated massive and laminated sandstone beds with medium to coarse-grained facies, and locally show scour erosive surfaces at the base of the main sandstone units. The sandstone beds have dip magnitudes up to 6°, easterly to northeasterly dip azimuth, and very rarely have southerly dip azimuth. The laminated sandstones locally show mud drapes. The SandTex patterns shows bimodal to poly-modal microresistivity histograms reflecting poorly to medium-sorted facies. Based on lithological and sedimentological characteristics as well as regional setting, the sandstone beds are interpreted as estuarine channel-fill sandstones. The prevalence of sandstone content in some packages reflects proximal setting to the influx of coarse clastics and sandstone supply. The associated silty heterolithics, laminated siltstone and mudstone point to deposition as estuarine mudstone at the top or in marginal setting of the estuarine channel. The brownish color fine-grained sediments indicate shallow-water depositional setting. The heterolithic and laminated deposits that occasionally occur within the estuarine units are likely to be sited laterally with respect to the more sand-rich channels, in the form of muddier, low-energy tidal channels or creeks cutting the marginal muddier areas of the estuaries (Thomas et al., 1987).

Generally, the sandstone is characterized by fining-upward tendency, an upward thinning of sets with variable thickness ranging between 1 m and 3.5 m thick. The sandstones with intraclasts are frequently recorded at the base of these sand bodies. The individual packages can be differentiated by dip magnitudes, azimuth of tadpole clusters, or both.

The recorded sandstone packages are separated by silty heterolithics, laminated and massive siltstone interbedded with laminated mudstone. The mudstone beds show easterly to southeasterly dip azimuth. This siltstone package ranges in thickness between 1 m and 2 m. The mudstones show greenish gray, dark gray, and yellowish brown colors based on mud log description (see Figure 11).

## Kafr El Shiekh Formation Depositional Facies Characteristics

### Submarine Channel Fill-Levee Complex

According to the biostratigraphic analysis, the base of this unit of the Kafr El-Sheikh Formation represents the contact between the Abu Madi and Kafr El-Sheikh formations. This contact shows an erosive planar surface. Nodular carbonate thin beds are recorded at the lower part. The sandstones lithofacies are composed of laminated massive sandstone and sandstone with resistive carbonate intraclasts (Figure12). Occasionally, the sandstone packages have a scour base and commences with sandstone with intraclasts. The sandstone lithofacies generally show easterly to southeasterly dip azimuth, with local northerly dip azimuth near the top. The dip magnitudes vary from 5° to 9°. The patterns show bimodal to polymodal microresistivity, indicating poor sorting index. In between these sandstone packages there are fine-grained sediments composed of massive claystone, siltstone, and laminated siltstone. Thin interbeds of argillaceous and laminated sandstone beds are identified at the upper part. These silty and clayey sediments show southeasterly to easterly dip azimuth, and their dip magnitudes range between 2° and 5°. The depositional motif of the sandstone, scour base, and presence of intraclasts at the base of sandstone packages point to submarine channel-fill sandstone.

They indicate deposition by high-density turbidity currents. The massive sandstone beds, lacking traction structures, point to deposition by surge-type turbidity currents in deepwater settings. The laminated sandstones commonly result from bed-load transport in the upper flow regime (Stow et al., 1996). The laminated sandstones are produced by surges of declining velocity in which sediments were worked as bed-load material prior to deposition (Lowe, 2004). The amalgamated stack of individual channel-fill sandstones are developed by continuous sand supply, where the fine-grained channel top is reworked. The intervening laminated siltstone, mudstone, and fine-grained sandstone reflect deposition in the proximal levee setting that flanks the channel-fill sandstones (Figure 13).

**Abandoned Channel Facies Association**

This depositional unit is commonly composed of massive siltstone and claystone beds. Occasionally, laminated siltstone and deformed mudstone beds (1-2 m thick) are identified. The laminated mudstone and the bed boundary of the massive mudstone and claystone show easterly to southeasterly dip azimuth. The dip magnitude of these fine-grained sediments varies from 5° to 15°. The dominance of massive fine-grained sediments reflects settling from suspension under quiet water conditions. This lithofacies represents abandoned channel deposits, which are developed during periods of low sand supply and flooding event, probably in mid-fan depositional suite.

**Intrachannel and Levee Facies Association**

This facies association is the basal unit in the studied succession. It is dominated by massive claystone and siltstone. This sedimentary unit comprises cross-laminated and deformed siltstone in low percentage. Thin- laminated and massive sandstone beds, ranging in thickness from 0.2 and 0.5 m, are rarely recorded. The laminated siltstone shows up to 10° dip magnitude and northeasterly to northerly dip azimuth in the lower and middle parts of this interval. However, laminated siltstone shows southwesterly dip azimuth in the upper part. The laminated sandstones display northwesterly dip azimuth and range in dip magnitudes between 2° and 10°. Silty heterolithics lithofacies (0.5-1.3 m thick) are recorded, where some laminae display wavy bedding and discontinuous to continuous mud laminae. Differential compaction is well recognized in the laminated siltstone as a result of compaction. The patterns display unimodal to bimodal microresistivity, reflecting a well-sorted to moderately sorted index. The massive siltstone and claystone point to deposition from suspension and slow fallout in low energy conditions. The laminated siltstone and silty heterolithics points to deposition by low-density turbidity currents (Al Siyabi, 2000). The local deformed siltstone reflects liquefied flows, where liquefaction results in disturbed sediments due to rapid deposition, storm waves, or both. The thin sandstone beds lack scour features and reflect a sudden increase in sand supply in overbank setting. This facies association is interpreted as intrachannel deposits and represents flooding and high-stand events in which little coarse sediment reached the basin. However, this sedimentary unit shows no direct association with submarine channels in the studied succession. If depositional facies correlation of the examined interval with surrounding wells shows a depositional relationship to nearby channel-fill sandstones, then it can be interpreted as distal levee facies.

**Channel-fill Sandstone Facies Association**

This facies association shows an increase in sandstone lithofacies. The sandstone beds are massive, thinly laminated, shaly, and occasionally with intraclasts. These massive sandstones and sandstone beds with intraclasts (Figure 13) as well as the laminated sandstone correspond to

Bouma Ta and Tb divisions, respectively. These sandstone packages have deeply scoured bases and a faint fining upward depositional motif. The scour bases are flat and recognized by abrupt vertical facies change. Their dip magnitudes vary from 2° and 5°. The dip azimuth of sandstone is generally directed toward the southwest, while it is locally directed toward the north. The dip magnitude of sandstone beds is generally around 5° and rarely increases up to 10°, which is attributed to local deformation close to the scour base. Dish-like structures and water-escape features are recorded in the shaly sandstone. The patterns show bimodal microresistivity, pointing to moderate sorting index. These sandstone packages are separated by laminated, cross-laminated, and massive siltstone as well as massive claystone. Occasionally deformed and slumped mudstone and muddy debrites are recorded. The cross-laminated siltstone corresponds to Bouma Tc division. The laminated siltstone and massive claystone are equivalent to Bouma Td and Te divisions, respectively. The massive sandstone and sandstone beds with intraclasts (Bouma Ta division) reflect deposition by rapid deposition by surge type, high-density turbidity currents in the upper flow regime. This interpretation is strengthened by the presence of fluid escape structures (Posamentier and Walker, 2006). Rapid deposition results in unstable initial grain packing. The recorded water escape and dish structures are produced by liquefied flow deposits (Al-Siyabi, 2000). The thin-bedded sandstone beds (Bouma Tbc divisions) were deposited by surges of declining velocity in which all sediment was worked as a bed-load material prior to deposition (Lowe, 2004). The laminated sandstones (Bouma Tb division) are traction-carpet laminations that are produced under lower energy of turbidity currents relative to Ta division. These sedimentological characteristics, fining-upward depositional motif, and scour base of sandstones reflect deposition from the bed loads of fully turbulent flows as submarine channel-fills. The upward variation in facies of the channel-fill sandstones suggests that the waning high-density turbidity currents evolved into depositing low-density flows. Bioturbation are recorded in the shaly sandstone, indicating intermittent quiescence periods to allow such faunal activity.

Carbonate concretions are identified as a diagenetic cementation in massive and laminated sandstone. These sand-rich submarine channels are cleanest and the highest net-to-gross facies in the field. The intervening massive siltstone and mudstone lithofacies represent Bouma Td and Te divisions and are the product of deposition from suspension. The cross-laminated siltstones (Bouma Tc division) result from fallout out of silt from suspension while lower flow regime; current ripples were moving on the bed (Stow et al., 1996). The cross-laminated siltstone shows southeasterly to northwesterly dip azimuth, and their magnitude ranges from 5° and 7°. A thick interval of fine-grained sediments represents abandoned channel deposits, which are developed as passive backfill of the channel. Thin beds of siltstone and mudstone reflect channel top deposits. They are developed by low-density turbidity currents during periods of decreased sand supply at the late stage of channel-fill immediately before channel abandonment. The prevalence of these fine-grained sediments is common mud-rich submarine fan system (Bouma, 2000), where they have low net-to-gross ratio. The recorded mud debris and slumped mudstones reflect mid- to upper-slope environments (Posamentier and Walker, 2006). These debrites are cohesive debris flow deposits, which are plastics and remain stationary once shear stresses can no longer overcome internal shear strength. They have no internal bedding or lamination and are commonly poorly sorted, where large clasts float in the matrix and sediments (Stow et al., 1996).

**Proximal Levee Facies Association**

This facies association is mostly composed of massive siltstone. Locally deformed, laminated, and cross- laminated siltstones, as well as thin beds of massive claystone, are recognized. They reflect deposition by low-density turbidity currents. The laminated siltstones show northeasterly and southwesterly dip azimuths, and their dip magnitude is up to 7°. The depositional setting and lithological characteristics point to deposition in proximal levee depositional suite.

### Distal Levee Facies Association

This thick sedimentary unit is dominated by massive and laminated siltstones. They are interbedded with thin beds of massive claystone. This laminated siltstone facies association shows absence an of scour base and cut-and-fill features. Most of the laminated siltstone shows easterly to southeasterly dip azimuth with local southwesterly dip azimuth. The dip magnitude varies from 3° to 20°. The patterns of siltstone show unimodal microresistivity, pointing to well-sorting index. Some intervals of laminated siltstone show development of stacked small-scale packages with downward decrease in the dip magnitude.

### Upper Bathyal to Outer Neritic Mudstone

This unit is dominated by massive claystone beds intervening with thin beds of siltstones. The basal bed of this facies association displays high gamma ray signatures, and its base is identified as a stratigraphic marker. The upper part of this sedimentary unit is dominated by massive claystone beds, which points to high sea level. These beds show southerly to southeasterly dip azimuth. Their dip magnitude is commonly up to 10°. The associated of this facies association show abundance of agglutinated and planktic foraminifera. This facies association represents open and deep-water hemipelagic deposits (background mudstone), which are likely to be deposited from suspension as background mudstone in outer neritic to upper bathyal setting.

## Conclusions

- The integration of the petrophysical evaluation, high-resolution microresistivity sand counting, electro-facies analysis, core data, biostratigraphy, and seismic data unveiled the ambiguities that previously existed, in particularly while characterizing Abu Madi and Kafr El-Sheikh reservoir facies (Figure 14).

- The paleocurrent analysis of channels in the Abu Madi and Kafr El- Sheikh formations in the field revealed the presence of northerly flowing slope channels.

- The sand count proved the presence of thinly bedded gas bearing reservoir in Kafr El-Sheikh, which has been confirmed by the pressure of an open-hole perforation test. This thinly bedded unit has increased the reserve estimate in the field.

- The general depositional facies in the field shows overall retrogradational patterns and a fining-upward depositional motif.

- The sandstone facies of the Abu Madi Formation in the field was interpreted as a sandy estuarine complex facies, which was deposited in the proximal setting to the sand supply and represents the best quality and cleanest facies.

- The sandstone facies of Kafr El-Sheikh Formation were interpreted as submarine channel fill/levee complex, and the thinly bedded gas-bearing reservoir was interpreted as interchannels proximal levee facies.

● The uppermost part of Kafr El-Sheikh Formation was dominated by claystone with minor siltstone interbeds. It represents open and deepwater mudstone that developed in upper bathyal to outer neritic depositional suite. Early Pliocene age is assigned to this mudstone-dominated unit, based on the presence of nano-plankton biozone.


## Aknowledgement

The authors would like to acknowledge GDF SUEZ staff for giving permission for publishing this article.


## References Cited


Al-Siyabi, H.A., 2000, Anatomy of a Type II turbiditie depositional systems: Upper Jackfork Group, Degray Lake area, Arkansas, *in* A.H. Bouma and C.G. Stone, eds., Fine-grained turbidite systems: AAPG Memoir 72, SEPM Spec. Publ. No. 68, p. 245-262.

Bouma, A.H., 2000, Fine-grained mud-rich turbidite systems: model and comparison with coarse-grained, sand-rich systems, *in* A.H. Bouma and C.G. Stone, eds., Fine-grained turbidite systems: AAPG Memoir 72, SEPM Spec. Publ. No. 68, p. 9-20.

Einsele, G., 2000, Sedimentary basins: evolution, facies and sediment budget: Springer, Berlin, 628 p.

Lowe, D.R., 2004, Deep water sandstones: Submarine canyon to basin plain, Western California: Pacific section AAPG Publications.

Posamentier, H.W., and R.G. Walker, 2006, *in* H.W. Posamentier and R.G. Walker, eds., Facies models revisited: SEPM Spec. Publ. No. 84, p. 397-520.

Stow, D.A.V., H.G. Reading, and J.D. Collinson, 1996, Deep seas, *in* H.C. Reading, ed., Sedimentary environments: processes, facies and stratigraphy: Blackwell Publishing, Oxford, p. 395-453.

Thomas, R.G., D.G. Smith, J.M. Wood, J. Visser, and E.A. Calverly-Range, 1987, Inclined heterolithic stratification: terminology, description, interpretation and significance: Sedimentary Geology, v. 53, p. 123-179.

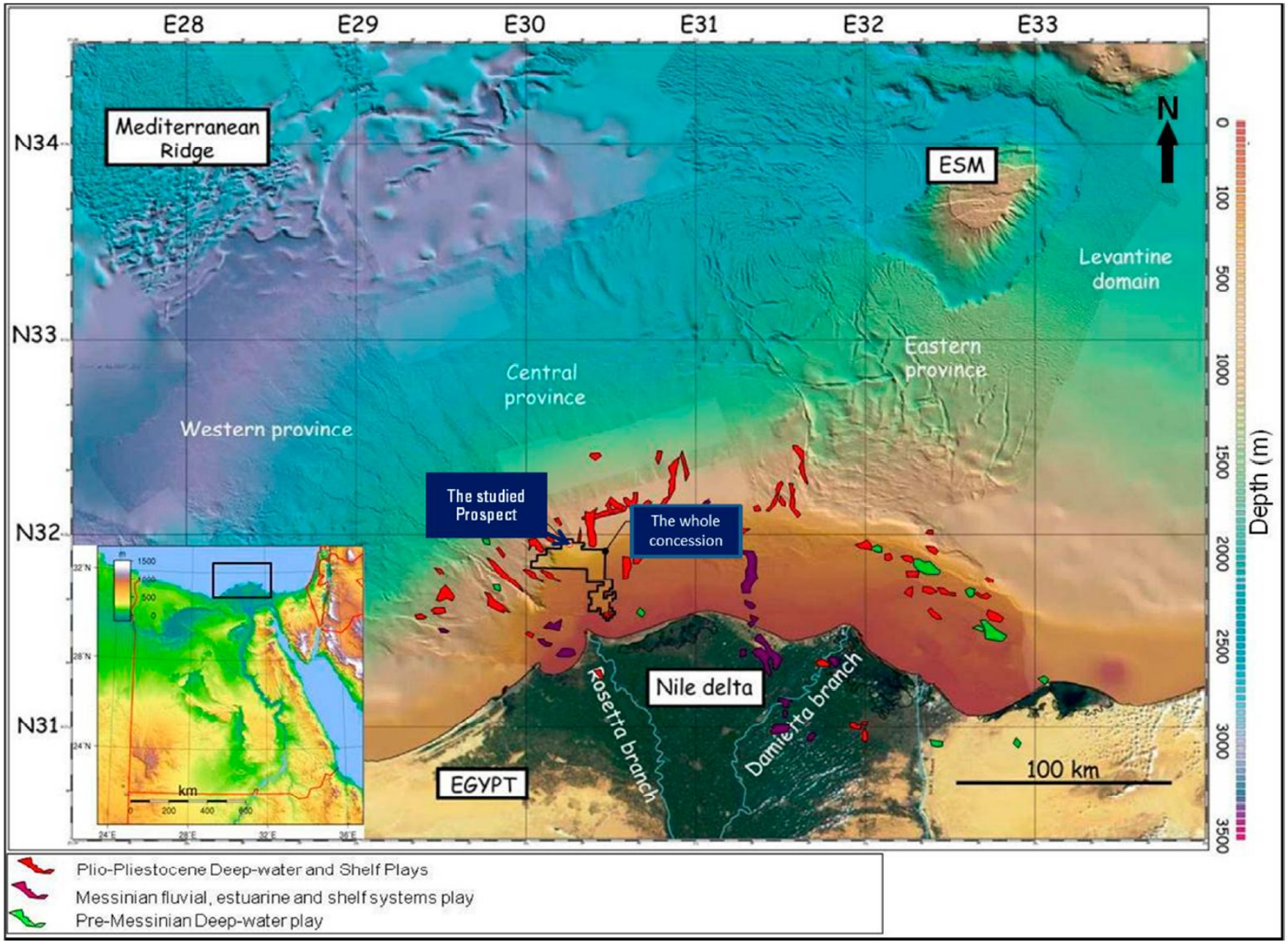


Figure 1. Location map of the studied prospect in west offshore Mediterranean of Egypt.

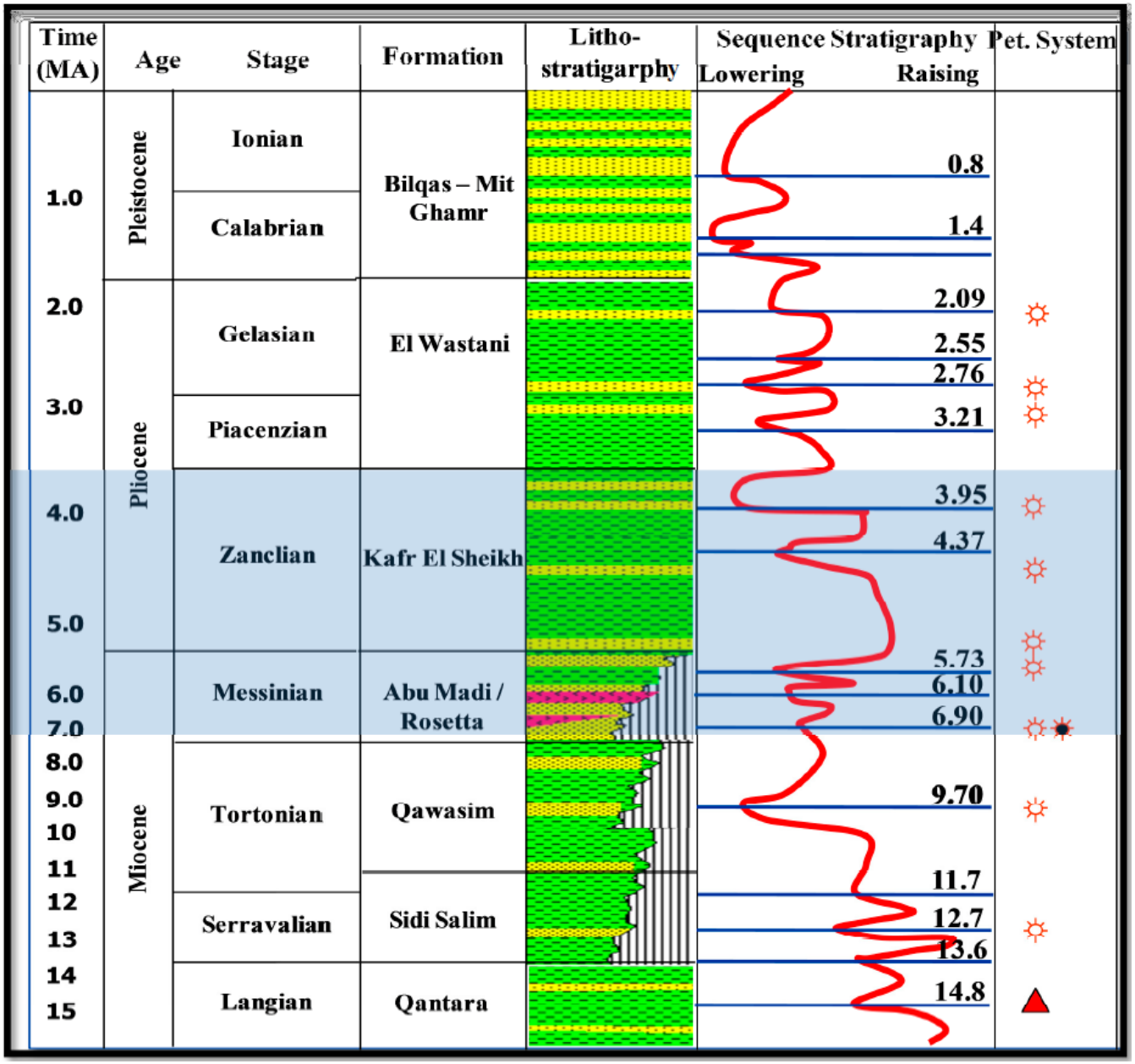


Figure 2. Western Nile Delta stratigraphic column with sea level curve. The target formations in the studied prospect are highlighted in light blue color.

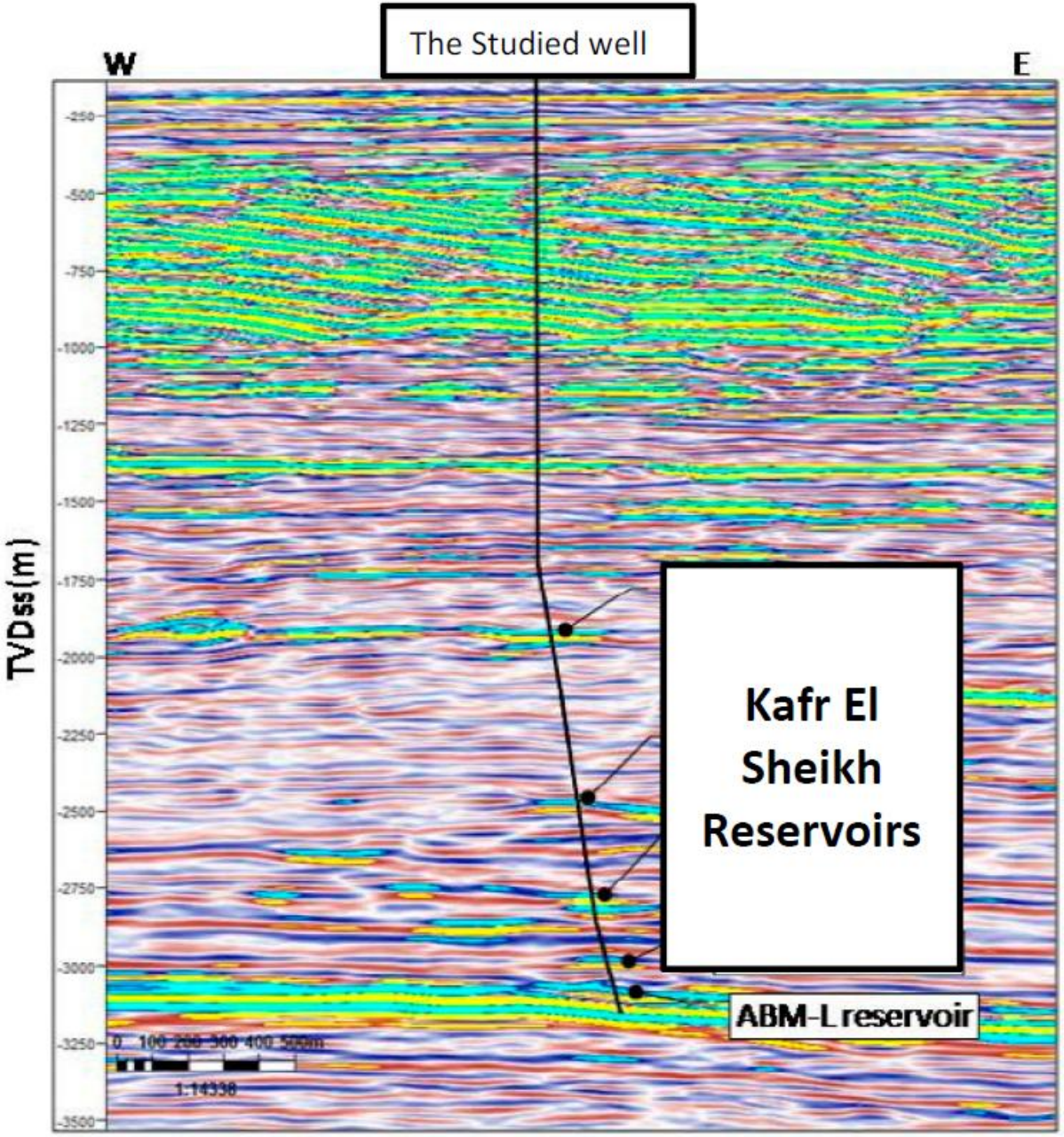


Figure 3. East-West full stack migrated seismic line passing through the studied well.

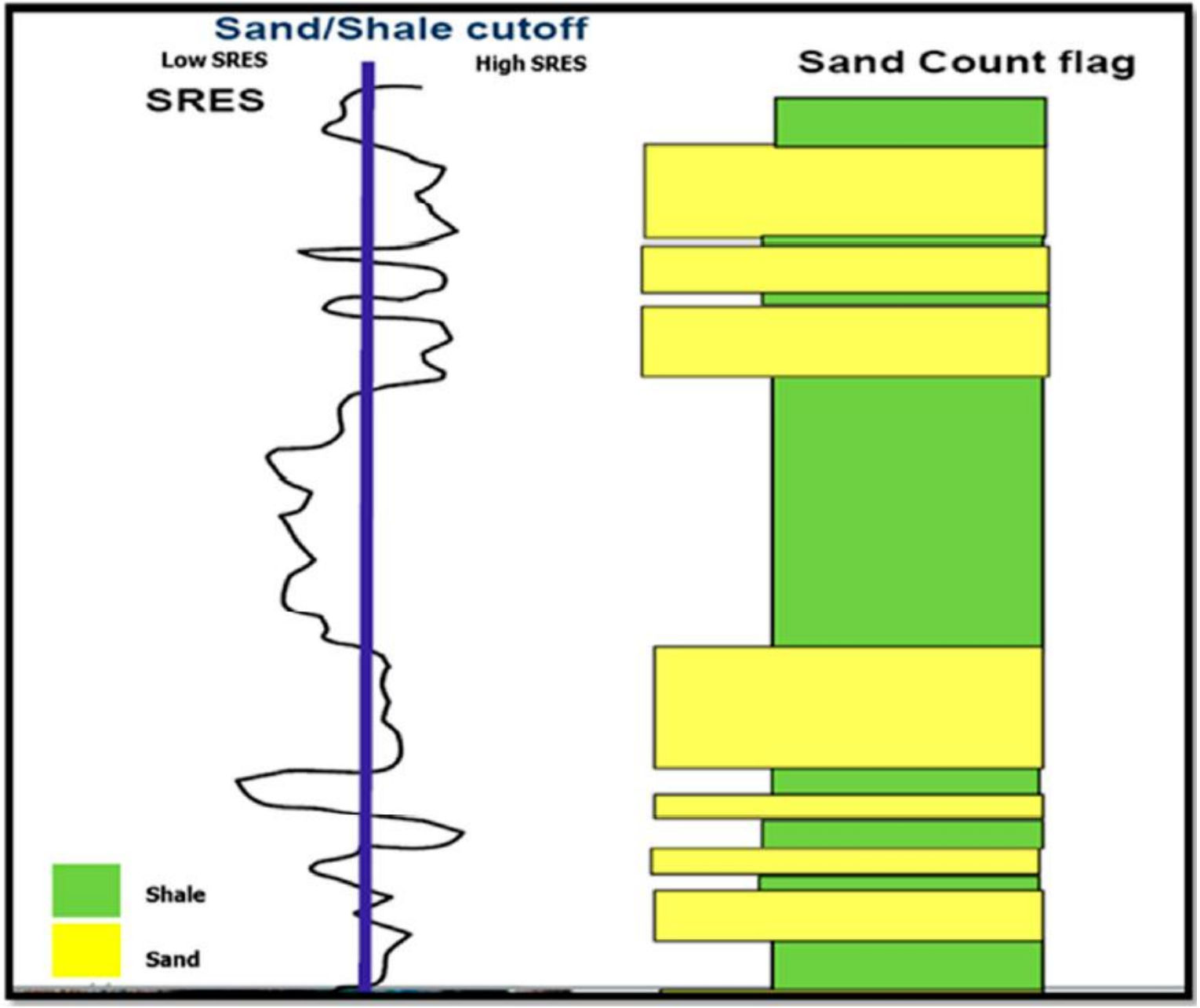


Figure 4. Basic concept of conventional sand counting method.

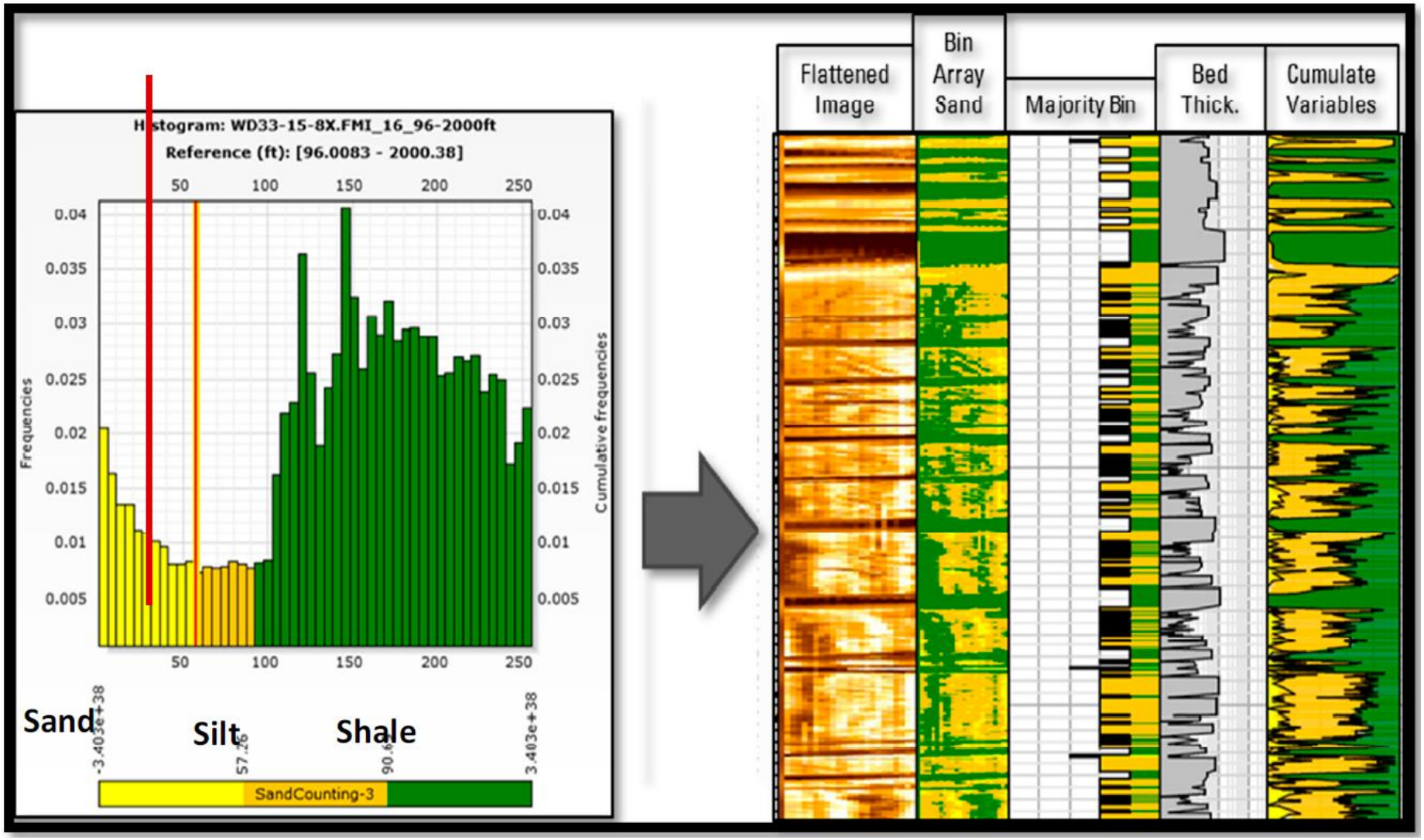


Figure 5. Statistical quantitative sand counting concept. Plot of the micro resistivity values displayed (left) in a histogram over a specific interval. Two cut-offs were used to differentiate among the clean yellow sand facies, the silty orange facies and the green shaly facies.

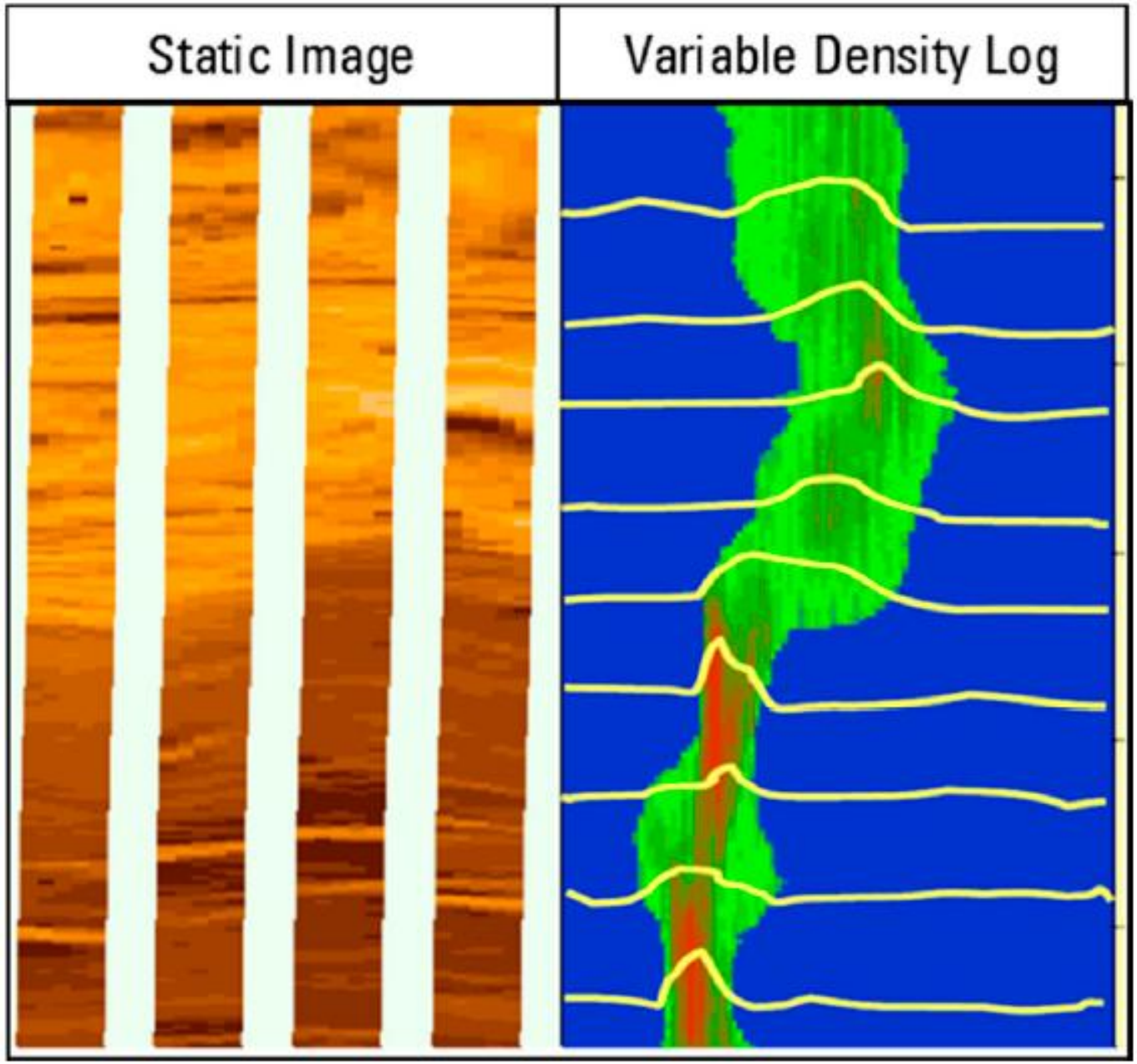


Figure 6. Image resistivity distribution viewed as a histogram or VDL display.

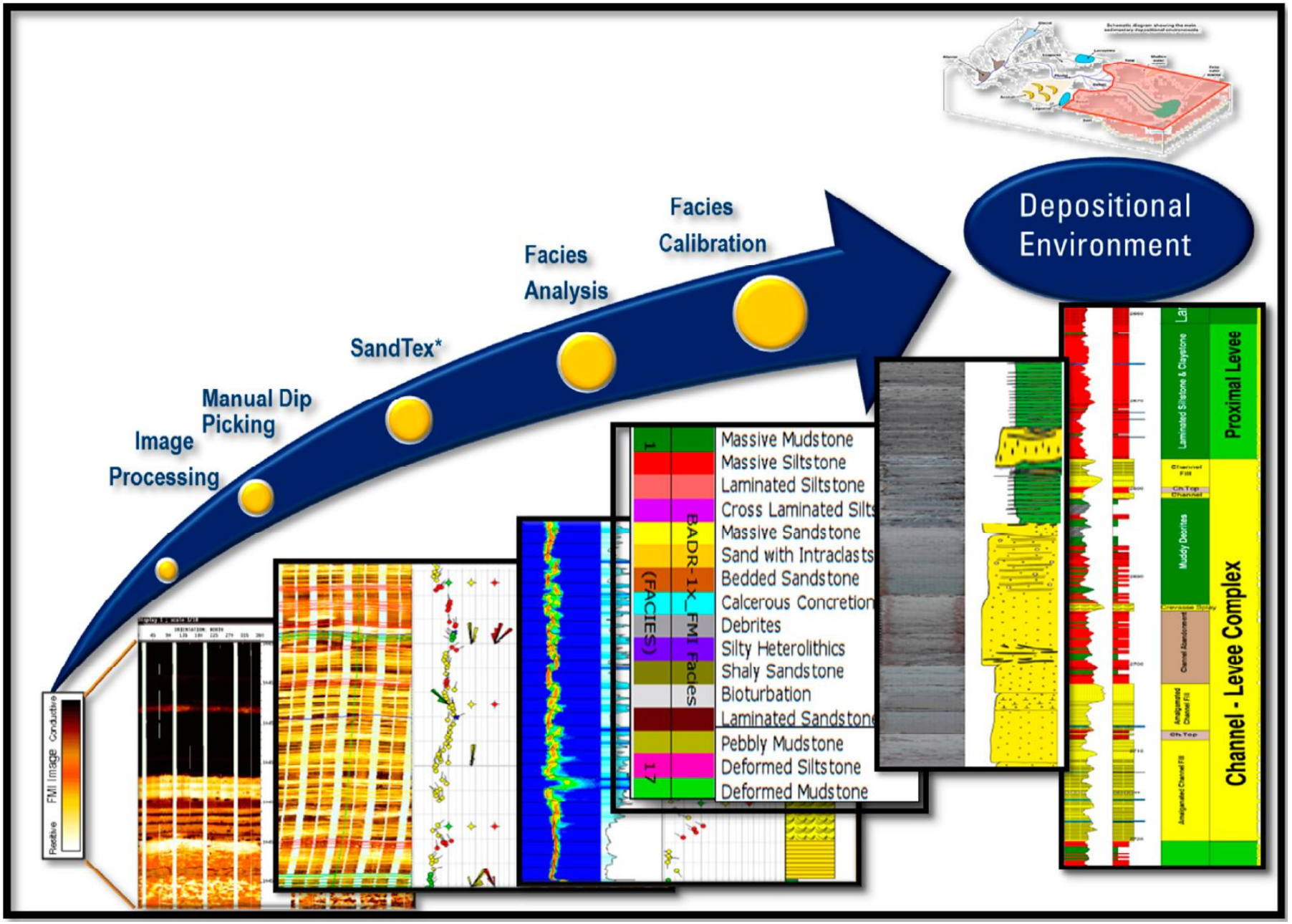


Figure 7. Summarized diagram shows the work flow of the Formation Micro-Imaging processing and sedimentological interpretation.

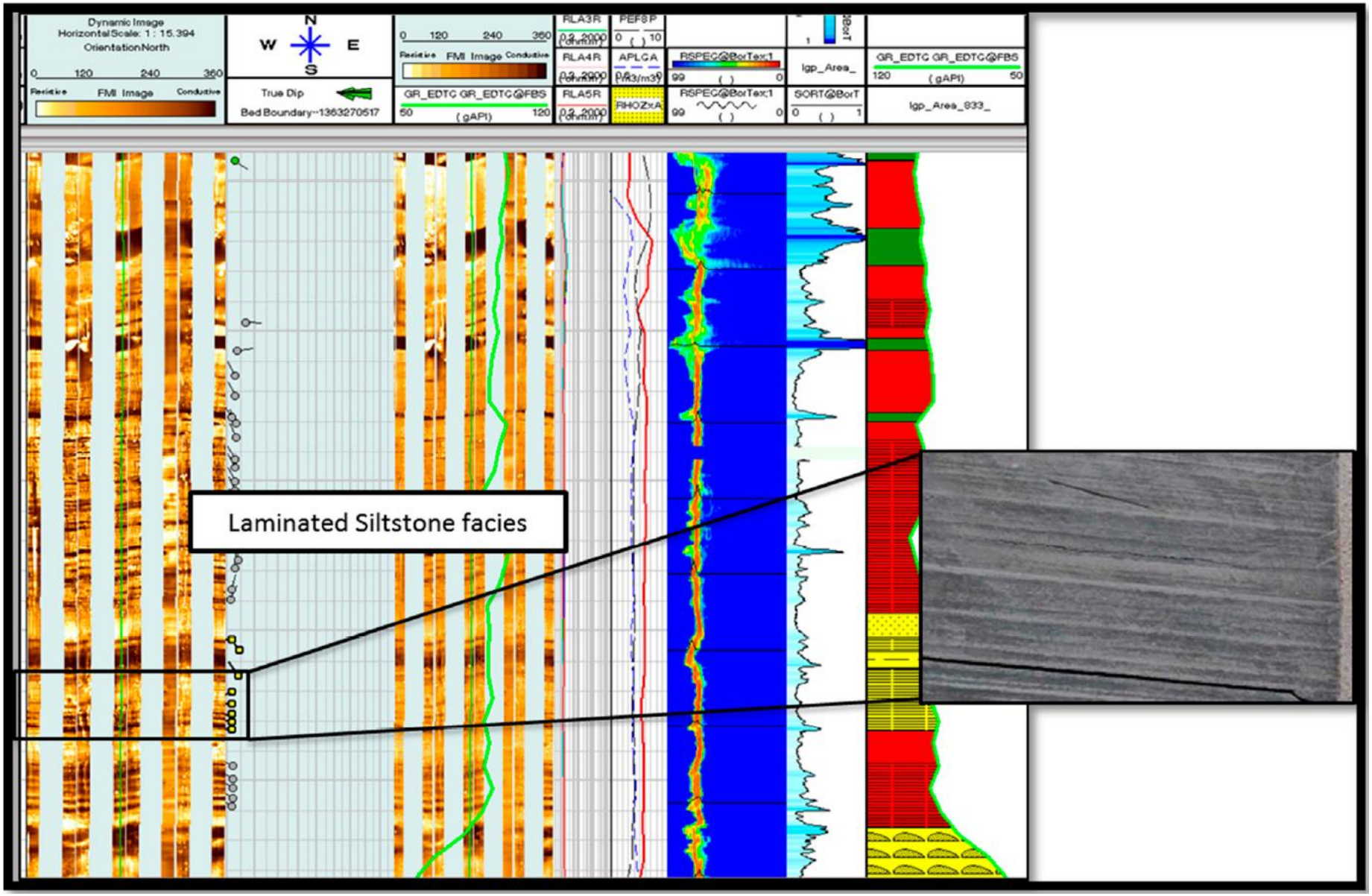


Figure 8. Example of laminated siltstone and sandstone facies seen in image and calibrated to the core.

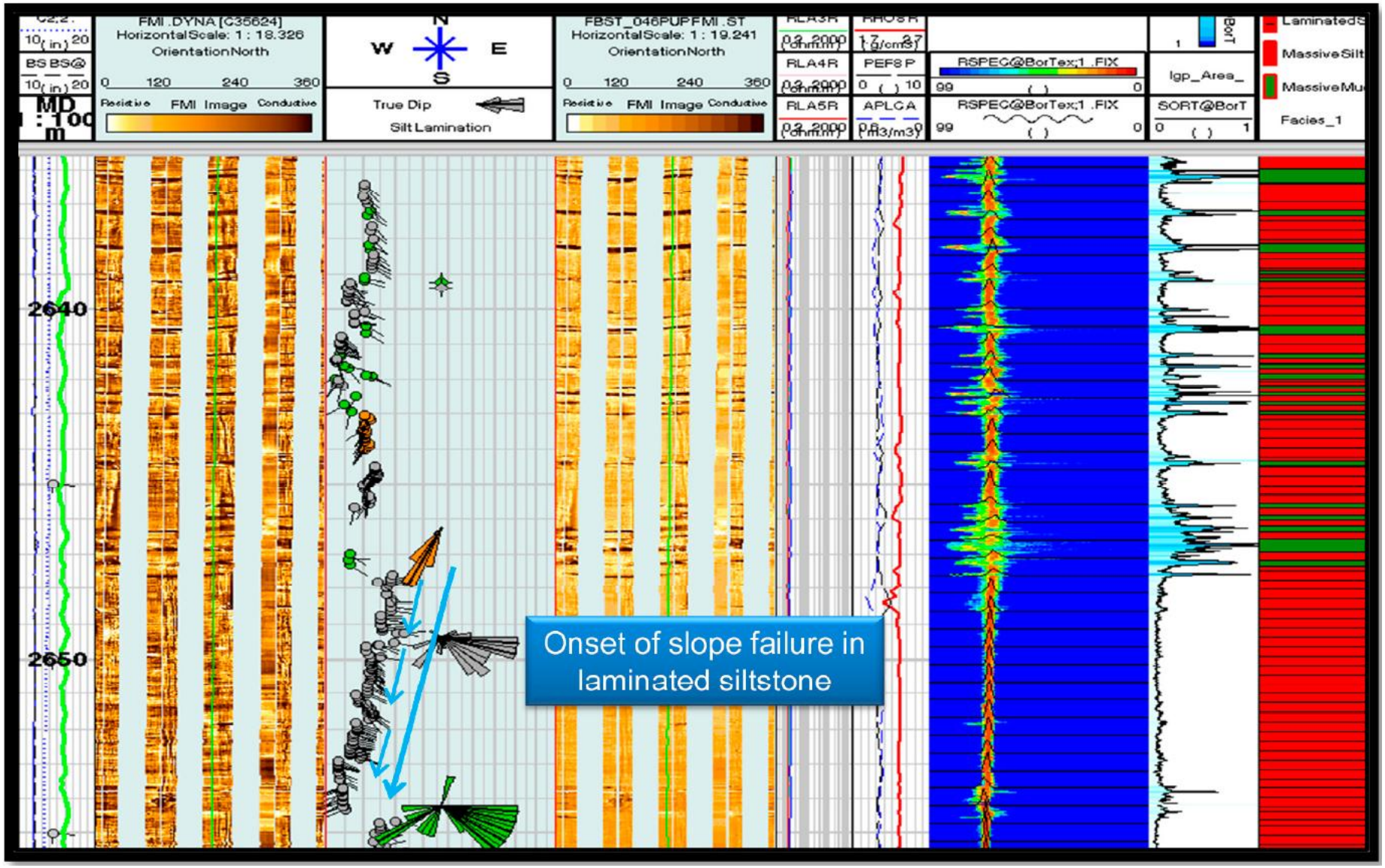


Figure 9. Laminated siltstone shows downward decrease in dip magnitude (blue arrows) as a result of increase in compaction or onset of slope failure.

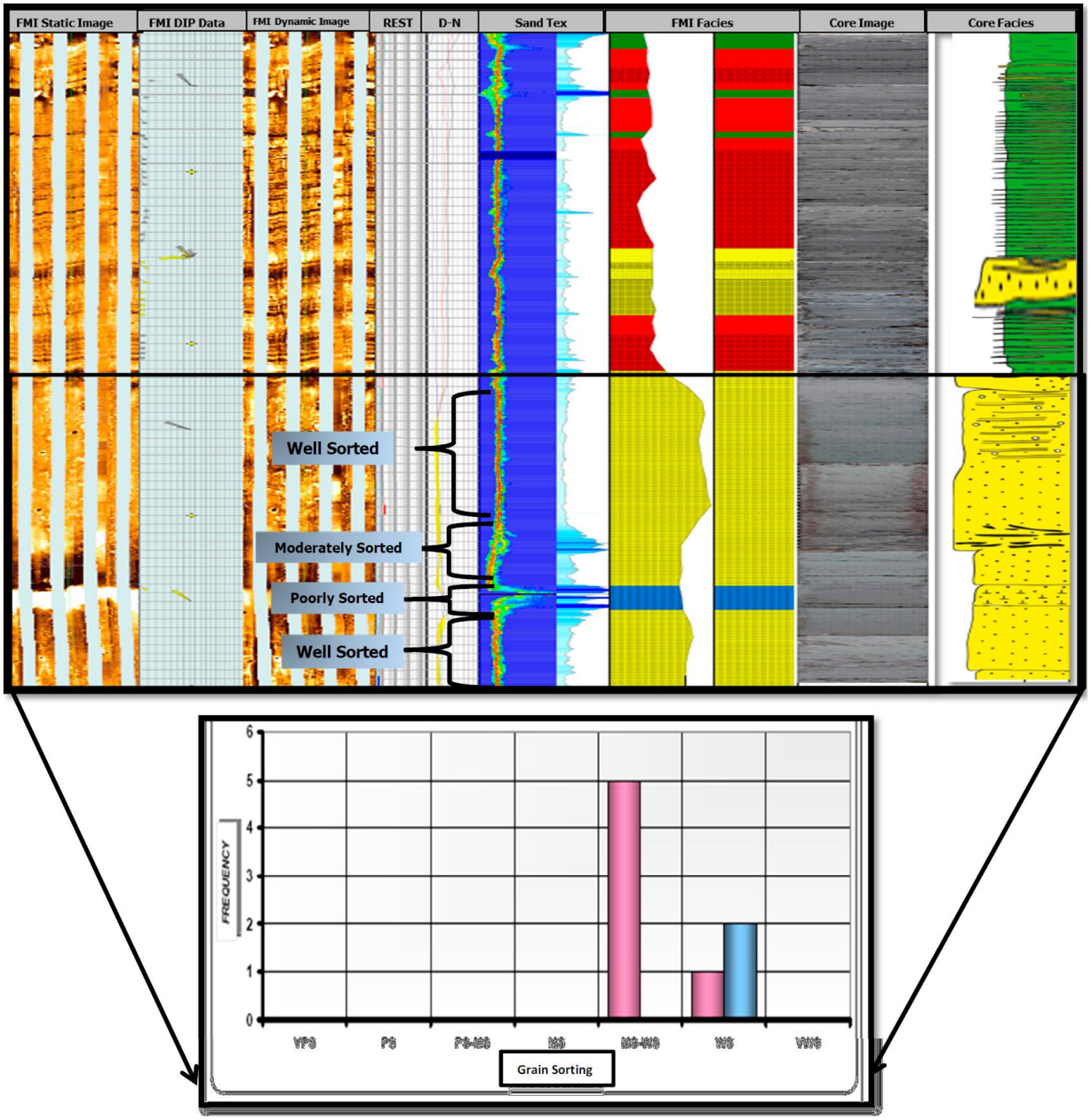


Figure 10. The sorting index generated from sand textural analysis and core grain size analysis; shows moderately to well-sorted sandy reservoir facies.

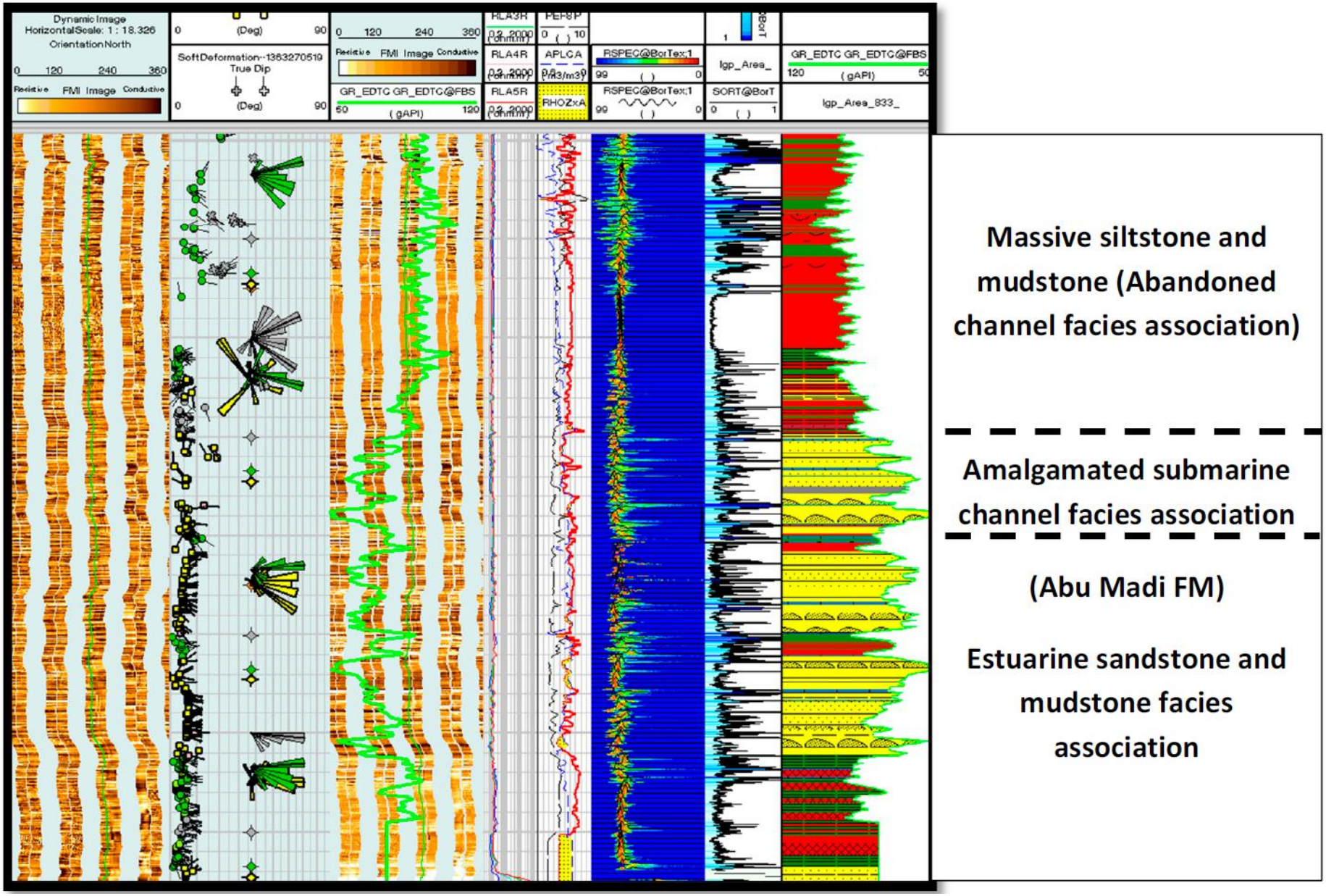


Figure 11. High-resolution micro-resistivity facies associations and their sedimentological characteristics (scale 1:300).

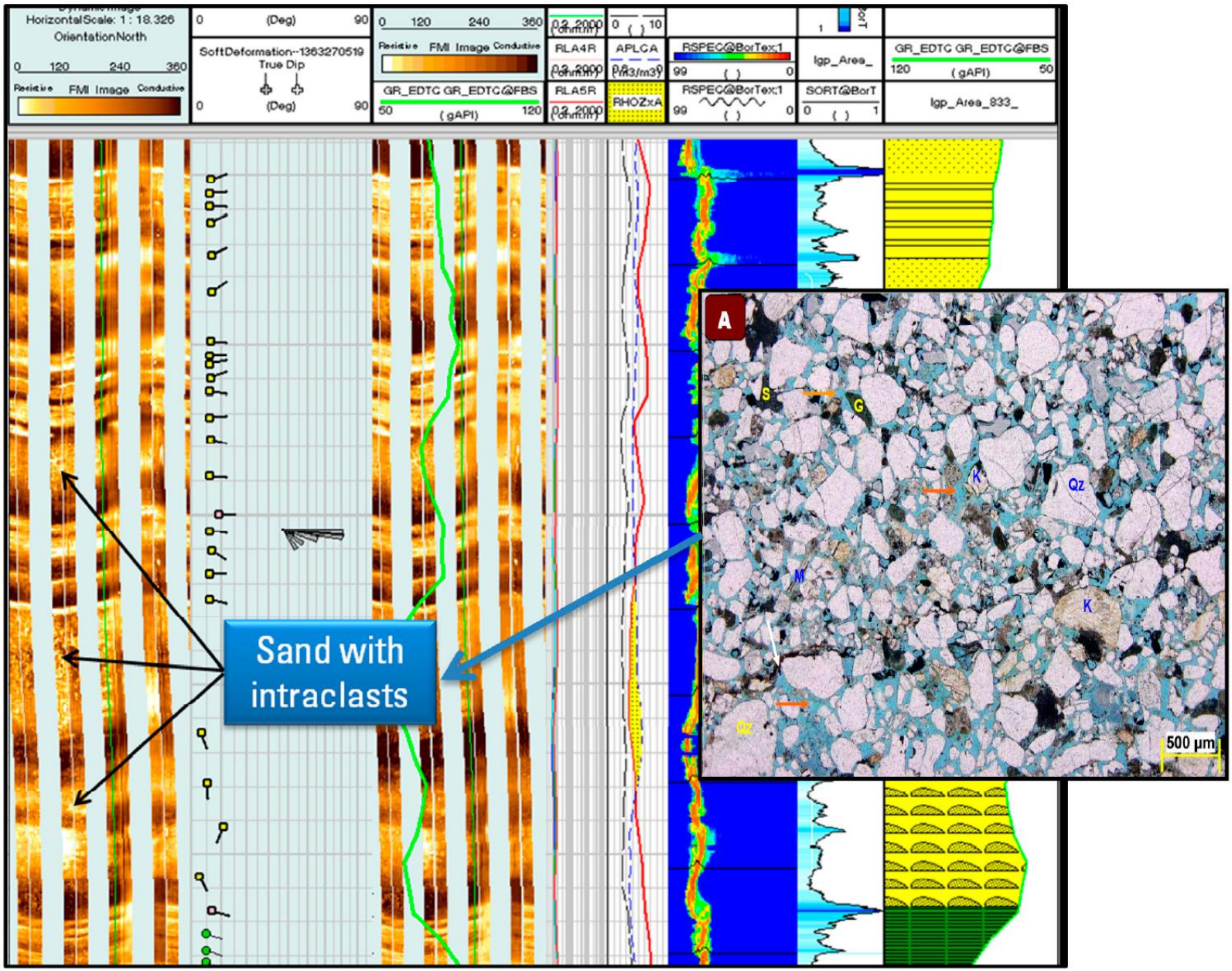


Figure 12. Estuarine channel-fill sandstones showing fining-upward tendency with intraclasts and a scour base. A microscopic thin section is also provided, showing medium to coarse-grained sandstone.

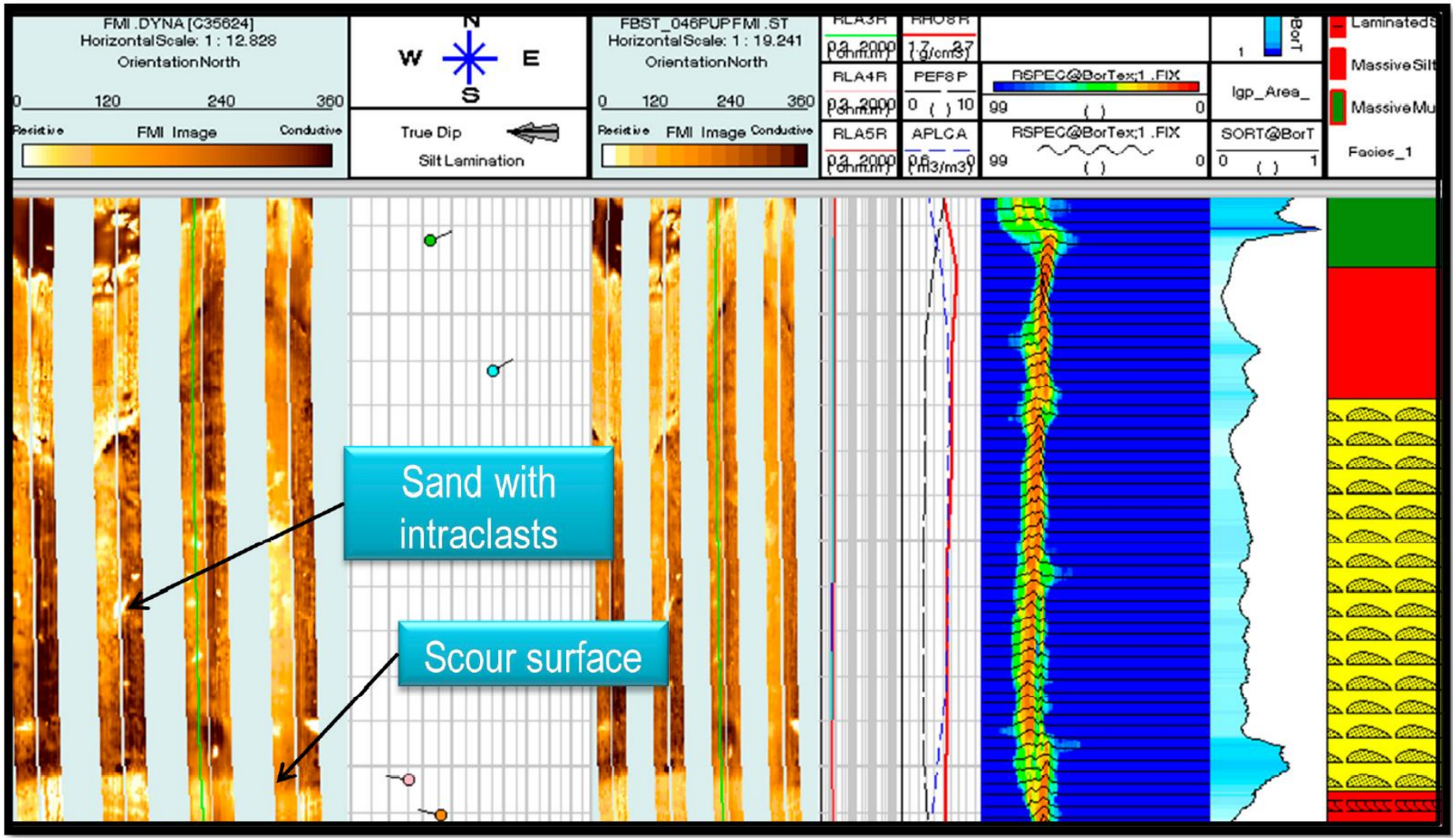


Figure 13. Massive sand with pebble-sized intraclasts with a scour surface at the base.

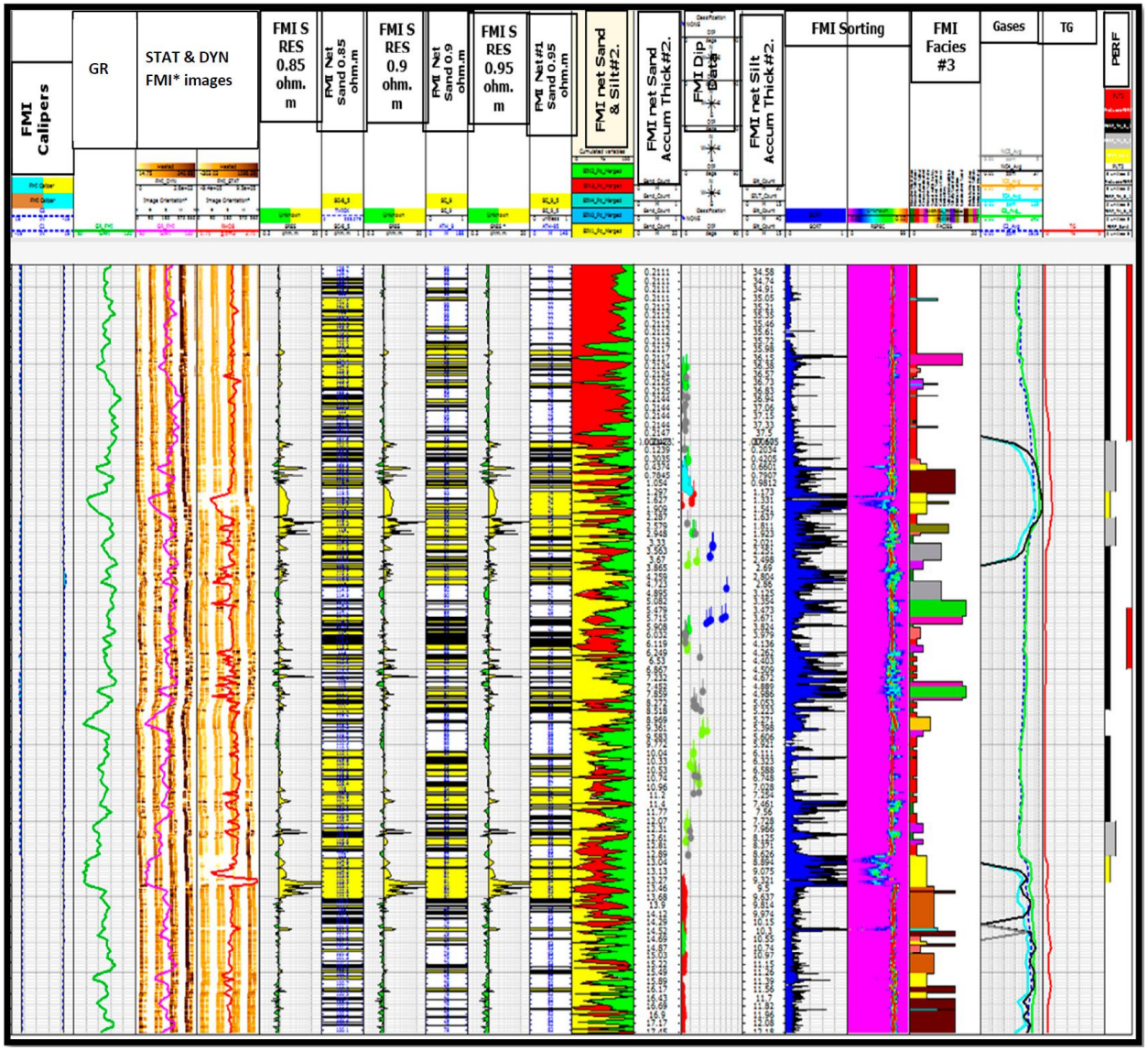


Figure 14. An integrated high-resolution micro-resistivity facies analysis and sand count composite plot in a section of the Kafr El Sheikh Formation showing the integration of the sand counting and facies analysis along with flag of the perforated intervals. The last track shows the perforated intervals in different colors. The black colour is the perforated intervals, the grey color is the areas separating the main sand bearing gas intervals and the thin bedded perforated intervals, the yellow color is the main sand bearing gas intervals which are not perforated, and finally the red color are the contributing intervals after running the production logging techniques (PLT).